Modeling the Metabolic Interactions of Astrocytes and Neurons
Under Normal Conditions and During Ischemic Hypoxia

Daniel Manson

March 2012

Abstract

It is relatively common for the brain of perinatal infants to be exposed to a period of reduced oxygen (hypoxia) and reduced blood flow (ischema). Left untreated, these episodes tend to cause permanent damage to the brain. In order to understand how this damage arrises and whether it is preventable, an extensive computational model has been developed that attempts to accurately capture the full metabolic complexity of the infant brain. This complexity encompasses everything from haemodynamics, to calcium channels in vascular muscle, to oxidative phosphorylation in the mitochondria of neurons. Model parameters are set using data from in vivo and in vitro experiments, as well as using a range of more ad hoc measures such as steady-state analysis. In the current model there is no distinction between astrocytes and neurons, i.e. the cell in the model is a rough average of the two. However there is plenty of evidence that astrocytes and neurons have quite different metabolic properties and interact in non-trivial ways. In this work we examine a separate model, designed for looking at the metabolic interactions of astrocytes and neurons, and examine whether any of its dynamics should be incorporated into the hypoxia model.

Contents

1 Biological Background

1.1 Cellular Respiration

[1] Almost all active processes in biology are powered by the following chemical reaction: [2]

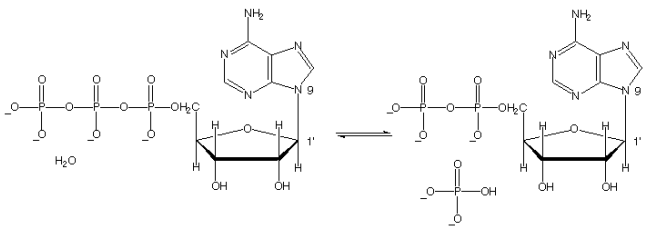

[1] The content of this section can be found in many textbooks including [16].
[2] Taken from [15].

The adenosine triphosphate (ATP) on the left is converted to adenosine diphosphate (ADP) on the right, releasing an inorganic phosphate ion (Pi) and energy. The reverse reaction, which endlessly recycles ADP to maintain the levels of ATP, takes place elsewhere in the cell using energy derived from an external source, e.g. ingested sugars. In this work we are interested in the ways in which ATP is recycled, and not so interested in cataloging all the different processes that consume it, though some processes will be relevant.

If ATP is the most important biochemical species, nicotinamide adenine dinucleotide (NAD^+) takes second place. As with ATP, the cell 'uses' NAD^+ in one location (or equivalently 'makes' NADH):

$$NAD^+ + 2\,e^- + H^+ \longrightarrow NADH$$

And in another location recycles the NADH. Here though it is not external energy that is required, but rather an external oxidizing agent to remove the electrons from NADH. When sufficient oxygen is available, it acts as the ultimate oxidizing agent, however under conditions of hypoxia it is pyruvate that acts as the oxidizing agent. As discussed below, the oxidation of NADH in mitochondria is in fact the most significant source of energy for the production of ATP.

Glycolysis This is the simplest method of ATP production and takes place is the cytosol of the cell. In essence, one molecule of glucose is split to produce two molecules of pyruvate, in the process phosphorylating two molecules of ADP to ATP. The reaction proceeds via several intermediary states, the details of which are not particularly relevant here. However it is important to note that the process uses two molecules of NAD^+.

The tricarboxylic acid (TCA) cycle The pyruvate produced by glycolysis enters the mitochondrial matrix, where it is used in the TCA cycle (also known as the Krebs or citric acid cycle). Again, the details are rather complicated, but essentially each pyruvate is split into three CO_2 molecules and in the process produces one ATP and uses four NAD^+.

Oxidative phosphorylation The NADH molecules produced by glycolysis and the TCA cycle transfer their electrons to oxygen.[3] This transfer is not direct, but progresses via several intermediary species embedded in the matrix membrane. At each step, the energy released is used to pump H^+ out of the matrix, resulting in the build up of an electrical potential across the membrane. Not until the energy has been stored in this electric field can it be used for the production of ATP. This is done by a trans-membrane enzyme - the ATPsynthase - which is a tiny electrical motor, literally rotating as a current (of protons) passes through it. Ultimately, it is the rotations of this enzyme which efficiently turn ADP into ATP.

For a highly simplified schematic of the above processes, see Figure 1. In addition to these methods of producing ATP from glucose in the blood, the cell employs a range of mechanism to buffer both glucose and ATP. This ensures that in times of reduced glucose or reduced oxygen, or in times of increased ATP usage, the concentration of ATP in the cytosol will never fall too far.

Glycogen Many animal cells store excess glucose as large globular polymers called glycogen.[4] Breaking down the glycogen does not require oxygen and produces the first intermediary species in the glycolysis pathway (glucose 6-phosphate) rather than glucose itself, saving one molecule of ATP. In muscle cells, this makes it effective for meeting a sudden increase in glycolysis during periods of intense activity. Indeed one of the functions of the mammalian liver is to store glycogen and make it available to muscles for such periods as this. However, there is a significant difference between muscle tissue and brain tissue: the activity of muscle cells is highly correlated, whereas the activity of brain cells

[3]The NADH produced by glycolysis does contribute to the proton gradient, but it cannot enter the mitochondrial matrix, so it has to pass its electrons to an intermediary carrier. Outside of the brain the carrier is malate, and the process is called the malate shuttle. However, in the brain the process may be simpler, with electrons being directly deposited in one of the trans-membrane enzymes. This pathway is called the glycerol 3-phosphate shuttle, and is less efficient at producing ATP but presumably more efficient at recycling NAD^+.

[4]Actually glycogen has a special protein at its core, so strictly speaking it is more than a simple polymer made of glucose residues.

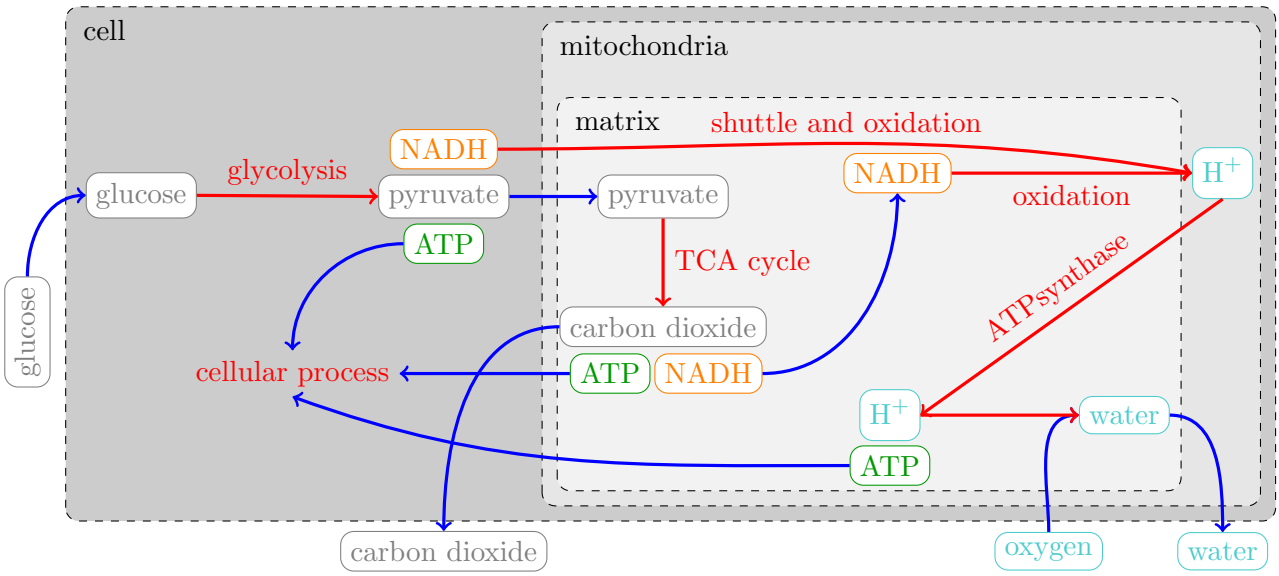

Figure 1: The schematic shows how, under normal conditions, glucose and oxygen are consumed by the cell in order to produce ATP, with carbon dioxide and water being the waste products. Red arrows represent active processes, and blue arrows represent movement of species (which in some cases is also an active process). The recycling/use of NADH and ATP, as discussed in the main text, is not shown here.

is not. This explains why muscles operating normally can create locally hypoxic conditions, but the brain will not. We will return to this point in the discussion of astrocytes and neurons.

Adenosine monophosphate (AMP) As well as the tri- and di- form of adenosine phosphates, there is a mono- form, which is a waste product of some cellular processes (rather than ADP). Conversion between the three forms is an important regulatory mechanism carried out by a specific enzyme (called adenylate kinase):

$$2\,\mathrm{ADP} \rightleftharpoons \mathrm{ATP} + \mathrm{AMP}$$

When ATP levels are low, the forward reaction is favored, restoring ATP levels to their target concentration. When ADP levels are low the reverse reaction is favored, thus making more ADP available to the ATPsynthase in the mitochondria. High levels of AMP will occur when the cell is struggling to meet ATP demands. In such circumstances the AMP concentration itself acts as a signal to reduce the rate of some of the less critical cellular operations, thus making more ATP available for the more critical operations.

Phosphocreatine Perhaps the most direct buffer of ATP is phosphocreatine, which takes part in the following reversible reaction:

$$\mathrm{phosphocreatine} + \mathrm{ADP} \rightleftharpoons \mathrm{ATP} + \mathrm{creatine}$$

When ATP demand is low the equilibrium shifts to the left, and when demand increases it shifts to the right, releasing the 'stored' ATP in a short space of time.[5]

1.2 Astrocytes and Neurons

It is a well known fact that neurons are responsible for transmitting, processing, and storing information. However, neurons in fact make up less than half of the cells in the mammalian central nervous system.[6] The remaining cells, which are known as glia, are diverse in morphology and function. Fig-

[5]The reaction has to be catalyzed by an enzyme (creatine kinase).

[6]This statement is true specifically for mammals; other taxa do have glia but there is some debate as to how closely related they are to mammalian glia - see [11] for a comparison with glia in drosophila.

ure 2 shows all three main types of glia, but in this work we are interested only in astrocytes since they are the most numerous and most relevant to metabolism during hypoxia.

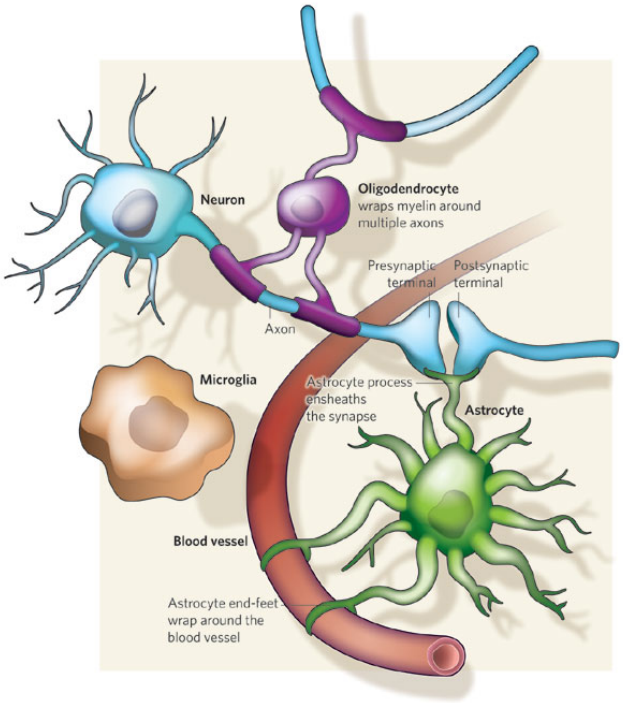

Figure 2: Cartoon showing different types of glia. Microglia are, as their name suggests, smaller than astrocytes and oligodendrocytes, which are the other two types of glia. The microglia act as the immune system in the brain, a role which exists because normal immune cells cannot cross the blood brain barrier. The oligodendrocytes produce myelin that electrically insulate the axons of neurons, so they are present only in the white matter. Astrocytes, which are discussed in the main text, exist in both grey matter and white matter. Taken from [1].

Like some neurons, astrocytes are stellate in morphology, making contact with tens of thousands of cells in a small area. However in astrocytes, these highly branched processes are neither axons nor dendrites, i.e. they do not conduct signals in the same way as neuronal processes. The contacts made with neurons are primarily at synapses, where the astrocyte is in contact with both of the neurons and the synaptic cleft. In addition to this extensive arbor of prcesses, most astrocytes also have 'endfeet' (shown in Figure 2) which wrap tightly around the brain's blood vessels. In particular they contact the cells which control the diameter of the blood vessels: smooth muscle cells (in the case of arterioles) and pericytes (in the case of capillaries). Astrocytes, unlike neurons, are connected to each other via numerous gap junctions that allow the mixing of cytosolic fluid. While this is clearly important, there also appears to be a degree of autonomy exhibited by the ends of each astrocytic process.

Investigation of the different properties of astrocytes is very active at the moment, with significant new functionality being discovered every few years (see [26] for a recent review). Here however, we focus primarily on metabolic function.

As mentioned in the previous section, for all cells in the body it is important that the level of ATP never drops too low. In most cells this is successfully prevented through a combination of glycogen, AMP, and phosphocreatine pathways. However, in neurons the ATP demand fluctuates over such a wide range that it cannot be met with these three measures alone. Neurons do use AMP and phosphocreatine pathways, but they 'outsource' the task of storing glycogen to neighboring astrocytes. This arrangement makes some intuitive sense given that each astrocyte contacts thousands of neurons and thus will have a relatively constant by-proxy energy demand overall.[7] To understand the neuron-astrocyte interaction in more detail, we now consider what occurs at a single synapse during a peak in neuronal activity.[8]

[7]Glucose is required for synaptic plasticity as well as general ATP production, but since synaptic plasticity is mediated by astrocytes there is again an intuitive sense in which astrocytes are well placed to provide the glucose.

[8]This discussion applies only to glutamatergic (excitatory) synapses, which make up more than half of the synapses in the mammalian brain. Less is understood about neuron-astrocyte interactions at other kinds of synapse. In fact it has been suggested [20] that inhibition requires less energy than excitation, and thus does not need astroycitic intervention in the same way.

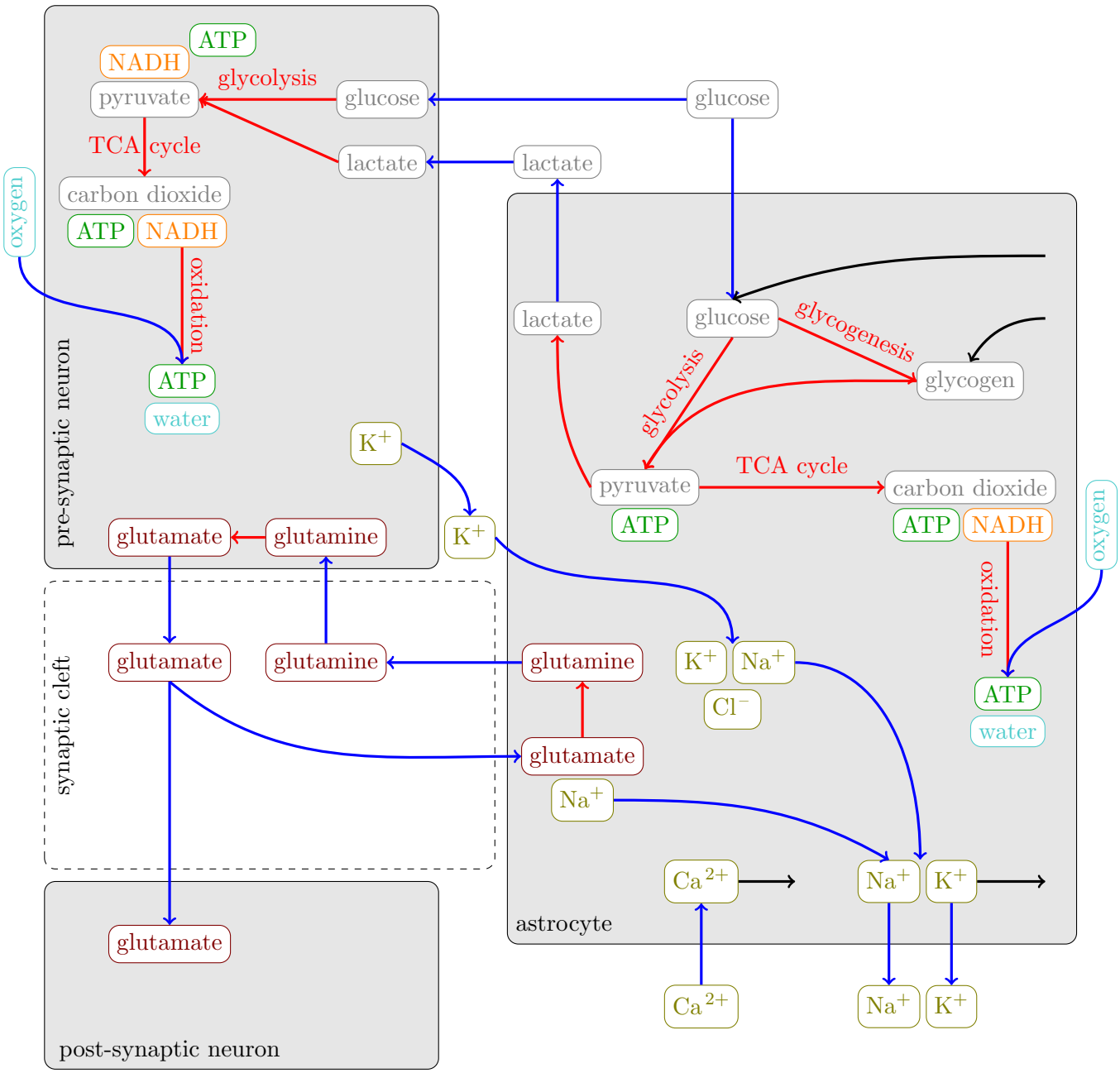

Figure 3: The schematic shows some of the neuron-astrocyte interactions under normal conditions. As before the red arrows indicate a process, and the blue arrows indicate a transfer (some of which are ATP driven). The black arrows show transfer to and from the rest of the astrocyte, and in particular its endfeet. Although the schematic depicts two separate networks, it should be understood that there is of course a strong bi-directional coupling.

A spike reaching the synapse of the pre-synaptic neuron causes a release of K^+ ions into the extracellular space, followed subsequently by a release of glutamate into the synaptic cleft. This glutamate is then able to act as a signal to both the post-synaptic neuron and the astrocyte. In the astrocyte however, glutamate uptake is more than a signal, it plays an active role in quickly restoring the extracellular glutamate levels to their pre-spike level as well as helping the pre-synaptic neuron to maintain a steady supply of glutamate vesicles. Both these aims are achieved by turning glutamate into glutamine, which deactivates its signaling properties and allows it to be returned to the extracellular space for re-uptake by the pre-synaptic neuron. The conversion to glutamine requires one ATP.

As with glutamate, the astrocyte is charged with restoring the extracellular K^+ concentration to

its pre-spike level. This is achieved by taking in K^+ through inward rectifying (one way) channels and through the $Na^+/K^+/Cl^-$ co-transporter. Having crossed the astrocyte's membrane, the K^+ diffuses through the astrocytic cytoplasm, to be released in regions of lower extracellular K^+ or into the blood at the endfeet. These processes are known as spatial buffering and spatial siphoning and are still a little controversial [26]. Since both K^+ uptake and glutamate uptake co-uptake Na^+, the Na^+ concentration within the cell increases. As with K^+, the increase in Na^+ diffuses through the astrocytic cytoplasm and is released back into the extracellular space elsewhere, in this case via the ATP-driven Na^+/K^+ pump. The transient increase in Na^+ concentration opens calcium channels in the astrocyte's membrane and causes a calcium wave to follow the Na^+ wave. There is some evidence that these two waves are detected at the endfeet, having an effect on the diameter of the blood vessel and perhaps on the rate of glucose uptake.

Back at the synapse, the glutamate signal triggers the astrocyte to start breaking down glycogen. As discussed in the previous section, the molecules cleaved from glycogen enter the glycolysis pathway and are converted to pyruvate. This all happens in the astrocytes, so the neurons do not benefit from the ATP generated. In order to help the neurons, the pyruvate must be converted to lactate and released into the extracellular space, where the neurons are then able to take it up. Once taken up by the neurons, the lactate is converted back to pyruvate at which point it can enter the TCA cycle (which produces almost no ATP unless oxygen is available). Thus, in hypoxic conditions the glycogen store is of no help to the neuron. Indeed if glycolysis in the astrocyte continues during hypoxia it will be contributing to the acidification of the brain. This is because each un-oxidised lactate is paired in solution with a proton (they are the dissociated ions of lactic acid). This whole system is referred to as the astrocyte-neuron lactate shuttle and over the last couple of decades has acquired a substantial amount of supporting evidence, though some questions remain [9, 19, 21].[9]

The above discussion is summarized schematically in Figure 3. We must note however that some points may not be relevant to neonates. In particular, the transporters that move lactate and glucose across the blood brain barrier, and into and out of cells, are expressed to different degrees in adults and the young. This allows neonates to use lactate directly from the blood, and perhaps reduces the role of astrocytes [9]. Interestingly, 70% of the newborn's body heat is generated by its brain [12], compared to a much lower fraction in adults.

1.3 Cerebral Autoregulation

In addition to the two levels of homeostatic functionality already described (buffers in the neuron and the astrocyte-neuron interactions), the brain as a whole also has a range of homeostatic mechanisms that attempt to maintain a constant blood flow and oxygen level. Figure 4 shows the resulting relationship between blood flow and pressure. The mechanisms involved have recently been discussed and reviewed in detail elsewhere [10], so here we just provide a brief summary.

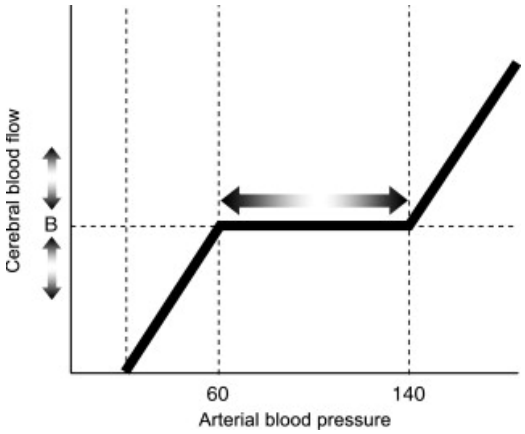

Figure 4: Units are mm Hg. *B* is the target flow rate, which can be maintained within the pressure limits shown. Data is for healthy adult. Figure taken from [10].

[9]For example, it is unclear to what extent oxidative and non-oxidative metabolism change during brain stimulation. What data there are do not seem to fully support the shuttle as described here, and may be better explained by a shuttle that uses lactate and pyruvate to transfer NADH to the neuron for oxidative phosphorylation.

- The anatomy of the blood supply to the brain is arranged so as to be able to maintain a relatively constant supply even if blockages occur in one or more of the arteries - see Figure 5.
- The diameter of the arteries exterior to the brain proper is controlled by nerves of the autonomic nervous system (whose cell bodies reside in the superior cervical ganglion, sphenopalatine, otic ganglia, and trigeminal ganglion).
- The diameter of the arteries entering the brain (i.e. within the parenchyma) can be controlled directly, and via astrocytes, by neurons from a specific set of nuclei (in the locus coeruleus, raphe nucleus, basal forebrain, and thalamus).
- The smooth muscle cells around the arterioles detect local changes in pressure and adjust accordingly to maintain flow.
- In addition to the K^+, Na^+, and Ca^+ signals already mentioned, changes in the concentration of ADP, ATP, CO_2 and a range of other molecules can cause dilations or contractions of arterioles and capillaries via G-protein-coupled receptors as well as via various other intermediary signals such as nitrous oxide.
- While the arterial flow rate and temperature are at normal levels, hemoglobin is able to maintain the correct oxygen concentration and pH value in tissue. This is known as the Bohr effect and works by shifting the equilibrium between the oxy- and deoxy- forms of hemoglobin: at high CO_2 concentrations or low pH values the deoxy- form is more stable and thus oxygen is dissociated and diffuses into the tissue, which ultimately increases pH.[6] However in ischemic hypoxic conditions un-oxidised lactate and CO_2 accumulate driving down the pH. Cellular buffers of pH do exist, but they are eventually overcome by rising H^+ concentrations, and when pH drops below 6.4 cellular function becomes impaired and eventually damage occurs [18].

1.4 Perinatal Hypoxia Ischema

In the developed world approximately 3-5 of every 1000 live births experiences some degree of brain damage due to hypoxia ischemia, with about half of the cases being fatal or causing severe damage to the brain (encephalopathy). It can occur during delivery if excessive blood loss occurs, but genetic or developmental abnormalities of the fetus are also commonly responsible.

It is thought that during the hypoxic insult some brain cells die via necrosis (uncontrolled death), but a comparable number actually die in the hours following the insult via apoptosis (programmed death) [12]. This apoptotic death has several likely causes including free-radical accumulation, and nitric oxide poisoning.

Cooling the neonate to around 34°C for several hours immediately after the insult has been shown to improve outcome to some extent. However, according to a recent meta-analysis [12] fewer than 1000 babies have so far taken part in long-term controlled randomized trials, making it difficult to accurately judge the benefit of the treatment.

2 Experimental data

2.1 Piglet in vivo

The piglet brain is considered to be a good model of the human neonatal brain (see [14] and reference within). Thus, simulating hypoxia ischema in piglets in the laboratory is a useful way of collecting a large amount of data under controlled conditions and without risk to human infants. The following types of measurements are possible:

Near-Infrared Spectroscopy (NIRS) Changes in oxy-, deoxy-, and total hemoglobin, as well as changes in the oxidation state of one of the enzymes in the mitochondrial matrix effect the brain's absorption of characteristic wavelengths of near-infrared light. It is possible to detect these changes by monitoring the absorption spectrum of near-infrared light passing through the brain (so long as the brain is small enough).

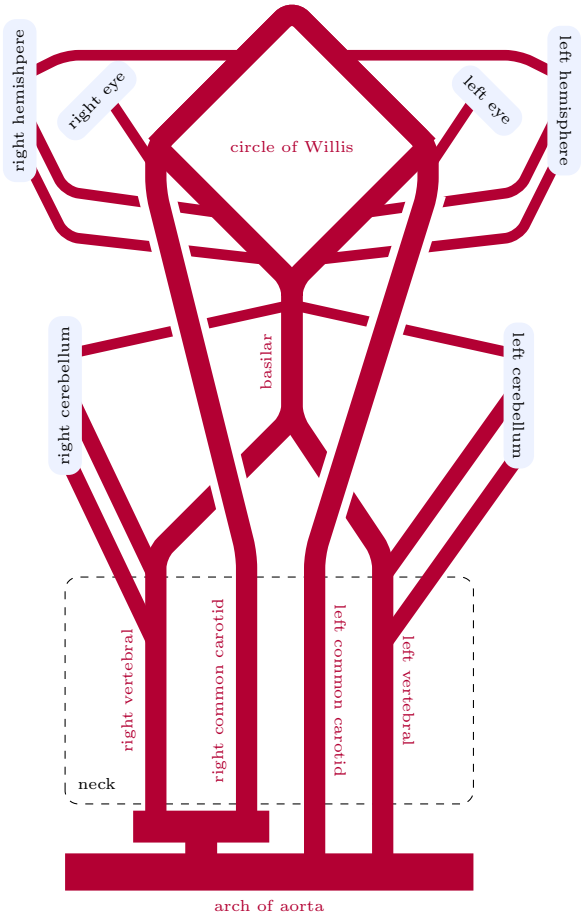

Figure 5: Blood has only a short distance to travel from the heart to reach the brain, however there are four major arteries through which it can flow. These arteries join at the base of the brain to form the circle of Willis, from which the cerebrum is fed. This arrangement ensures that if any of the feeding arteries is blocked the brain will still receive a reasonable supply of blood. Diagram constructed from figures in [23].

Magnetic Resonance Spectroscopy (NMR) Using large magnetic fields it is possible to measure the local electromagnetic environment of a particular type of particle within a sample. This can be done for hydrogen, carbon, and phosphor nuclei (though not at the same time) to produce a spectrum with second-level temporal resolution. Analysis of such spectra indicates the levels of each of the different phosphates (i.e. ATP, ADP, AMP, Pi and PCr).

Blood Pressure can be measured continuously and samples taken for detailed analysis every so often.

Breathing apparatus The levels of oxygen and carbon dioxide in the exhaled air can be measured.

Thermometer Temperature is measured, and also controlled by keeping the piglet in a waterbath.

2.2 Rat in vivo

While the piglet brain is useful for simulating the hypoxic brain in infants, if we just wish to examine cellular level processes it is easier to use a more primitive mammal, such as a rat [7]. With the rat we can collect the following data:

Microvoltametric electrode A mciroelectrode implanted in the rat brain oxidizes or reduces molecules in the extracellular fluid. Measuring the current at a range of voltages multiple times a second allows a measurement of the diffusion rate of molecules with different electrochemical properties. This makes it possible to calculate the concentration of extracellular species such as glucose and lactate, even in freely moving rats.

2.3 In vitro

The in vivo data is helpful, but has to be supplemented by in vitro measurements. These data, which are in most cases taken from general literature, give approximate values for enzyme, transporter, and ion channel dynamics. Given the limitations of in vitro experiments, the possibility of variation across species, across cell type, and across developmental stages, these data are only approximately applicable

in the case of the human neonate brain undergoing an hypoxic ischemic insult. (For example, see [6] for variations in hemoglobin properties across species and ages.)

3 Modeling

3.1 Important Classes of Equation

The hypoxia model and the astrocyte-neuron model discussed in the next section have been developed to model different aspects of the biology thus far discussed. Both models consists of a variety of equations, some of which are based purely on empirical evidence, but many are grounded in well-understood chemistry and physics. Here we discuss three such classes of equation.[10]

Mass Action For a simple chemical reaction, the law of mass action, which can be derived with statistical mechanics, states that the reaction rate depends only on the product of reactant concentrations, raised to the power of their stoichiometric constants. For example, for the reaction:

$$3\,\mathrm{A} + 2\,\mathrm{B} \rightleftharpoons \mathrm{C}$$

the rate of the forward reaction is equal to $k_1[A]^3[B]^2$ and the rate of the reverse reaction is equal to $k_{-1}[C]$, where k_1 and k_{-1} are constants. At equilibrium the two rates are equal, and so we find:

$$\frac{[A]^3[B]^2}{[C]} = \frac{k_{-1}}{k_1} = K$$

This is valid so long as the reaction progresses in a single step and the species involved are small and freely moving.

Michaelis-Menten Whether occurring in solution or at a membrane, many biological reactions require an enzyme and have the following form:

$$\mathrm{E} + \mathrm{S} \rightleftharpoons \mathrm{ES} \longrightarrow \mathrm{E} + \mathrm{P}$$

where E is the enzyme, S the substrate, and P the product. From this, one can derive the modern Michaelis-Menton equation, though the following two assumptions must be made: the concentration of the substrate is much higher than that of the enzyme; and the fraction of enzyme molecules with vacant binding sites does not fluctuate (i.e. the first part of the reaction is at steady state).

$$V = \frac{V_{\max}[S]}{K_m + [S]}$$

The equation gives the rate at which substrate is converted to product given the rate at high substrate concentration, $V_{\max}$, and a constant, K_m.

The derivation is not valid if the reaction is reversible or if it includes multiple substrates or multiple steps. However in practice it is often possible to apply it empirically, or derive a slightly more appropriate equation.

Nernst Changes in the concentration of ions on either side of a membrane are central to much of cellular biology, especially in the case of neurons and astrocytes. It is possible to derive a relationship between the membrane potential and the ion concentrations by considering the energy needed for an ion to cross the membrane and then calculating what fraction of the ions will possess the necessary energy. The energy required is simply $-zqV$, where zq is the charge on the ion and V is the membrane potential; and the fraction of ions with the necessary energy is $exp(zqV/k_BT)$ or equivalently $exp(zVF/RT)$, where T is the temperature and k_B, R, and F are the Boltzmann, gas, and Faraday constants. At equilibrium, the probabilities of crossing the membrane in either direction are equal, and we find:

$$V_{eq} = \frac{RT}{Fz} ln\left(\frac{[A_1]}{[A_2]}\right)$$

[10] These equations are given a much more complete treatment in [4, 16, 8].

where $[A_1]$ and $[A_2]$ are the ion concentrations on either side of the membrane. This equation is not valid for complex ion channels that let multiple ion species through or have voltage-dependent conductance.

3.2 Overview of modeling

Over the last few years, biological models have become increasingly complex, creating the need for both standardization and electronic databases of peer-reviewed models. The Systems Biology Markup Language (SBML) seems to be the current data standard, however it is evolving quickly and there are still many other formats in use for a range of specific modeling niches. In addition to variations in data format there also exists numerous different application programming interfaces (APIs) and graphical user interfaces (GUIs).

Constructing a model from known biology is in principle relatively straight forward. One abstracts the system into a small number of compartments in which the concentration of chemical species and physical properties can be simulated using differential equations. The equations represent flow between compartments, flow in and out of the system, and chemical reactions that convert between species (as per the examples in the previous section). However this in itself is of little utility; meaningful values have to be found for all the parameters of the system, even those for which no experimental data is available (or relevant). A simple way of doing this is to set the parameters such that the variables (also known as 'states') converge on steady state values with reasonable magnitude (this is known as flux balanced analysis). Additionally the model can be calibrated by minimizing a prediction error relative to an experimental data set.

The resulting model can be given a range of initial conditions or time-dependent conditions, from which it will predict a set of outputs. However, whether or not these outputs are meaningful is difficult to say, especially if the model is operating in a region of parameter space far from where it was calibrated. Failure of accurate prediction could be caused by inaccuracies in the parameters or - as is common in complex biochemical systems - by different phenomena being active in different regions of parameter space.[11]

Here we look at two separate models. The first model simulates hypoxic ischema in piglets (the Moroz-Banaji model [14]), and the second model simulates the neuron-astrocyte interactions in rats (the Cloutier model [7]).

3.3 Moroz, Banaji et al. Model

This model was built using the BRAINCIRC environment. As shown in Figure 7, the model has a compartment for the arteries, capillaries, veins, and a pair of generic-braincell compartments for cytoplasm and mitochondria. It was designed to simulate a range of experimental data sets obtained by inducing hypoxic ischemia in piglets (as discussed earlier). In constructing the model, the modelers chose where possible to represent only experimentally observable quantities.

The circulatory component of the model allows for dynamic changes in venous and arterial volume driven by changes in oxygen concentration. Changes in arterial volume translate to changes in hemoglobin, which in turn translate to changes in the rate of oxygen delivery to tissue. The arterial oxygenation of hemoglobin is provided as an input time series, as is the partial pressure of oxygen in the arteries. Using these inputs the model was used to predict a range of outputs that showed strong qualitative agreement with experimental data.

[11] When dealing with large models of many parameters it is often necessary to run the model many times using different parameters and initial conditions, this permits an analysis of parameter specificity and solution stability. However running the model many times requires that the model execute relatively fast while maintaing accuracy over the full time course. The simplest method of numerical integration, incrementing each variable by its numerically evaluated derivative (the forward Euler method) becomes significantly less accurate as the time step is increased. So instead it is common to use a more complicated method (the backward Euler method) which numerically evaluates the derivate at possible future values and then chooses the value which best agrees with the current value, i.e. $x_{n+1} = x_n + hf(x_{n+1})$ rather than $x_{n+1} = x_n + hf(x_n)$. In some circumstances it is also helpful to combine the two methods (the Crank Nicholson method).

Various combinations of parameters are subjected to a steady state analysis and a comparison is given with a version of the model adjusted for more adult-like parameters.

3.4 Cloutier et al. Model

This model was built using the Systems Biology Toolbox for MATLAB. Its 34 differential equations simulate the astrocyte-neuron metabolic interaction in a healthy, freely moving rat. Figure 8 shows the full model which consists of four compartments: an astrocyte, a neuron, an extracellular space, and a capillary. This model extends an older astrocyte-neuron model with the addition of the glycogen store in the astrocyte, a more detailed glycolysis pathway, and an explicit coupling of the neuron and astrocyte via the glutamate cycle.

The model incorporates a time-dependent stimulus variable which allows the modeler to examine how the coupled cells behave during stimulation, however it makes no attempt to capture the larger scale dynamics of either cell or the changes in local blood flow (except via an explicit time-dependent equation). As stated by the authors, the system is inherently at a non-steady state, so doing flux balance analysis is not entirely appropriate (and difficult to calibrate to experimental data for neurons and astrocytes separately). Instead the authors calibrate their model by minimizing the predicted error relative to experimentally obtained extracellular glucose and lactate time series (this process is aided by choosing reasonable initial values from the literature). The model resulting from this process is tested against further data and found to be of reasonable accuracy. One interesting asymmetry in the model is that astrocytes and neurons have different rate constants for various processes, notably the maximal mitochondrial rate of oxidation, which is higher in the neuron.

One of the important biochemical parameters not in the model is pH. However, in a separate paper [18] by different authors, some attempt is made to modify the Cloutier model to account for pH. See Figure 9 for the full modifications to model, which essentially consist of a set of H^+ dynamics explicitly tied to the concentrations of ATP, lactate and phoshocreatine, and a series of new channels for H^+ transfer. The modifications do include the effects of H^+ on CO_2 concentration (via the carbonate ion buffer), but still do not include any larger-scale effects on the blood vessels or the oxygen binding efficiency of hemoglobin. In addition, the glutamate coupling, despite being considered key in the Cloutier model, is not present in the modified version.

In addition to the Cloutier model there are at least two other astrocyte-neuron models in the literature. Both are provided here for convenience (Figures 10 and 11, [17, 5]). The second model is the most complex of all the models and is used by its authors to demonstrate the stability of various cycles, but it is not evaluated against any experimental time series.

4 Hypoxia Ischema and the Cloutier model

From the preceding discussion (and accompanying figures) it is apparent that the differences in the two models are almost as significant as the similarities and yet both models omit significant aspects of known and potentially relevant biology. To reiterate, the Moroz-Banaji model does not represent any of the neuron-astrocyte interactions or the glycogen store; and the Cloutier model does not allow for any changes in venous dynamics. The models also attempt to capture the dynamics of very different protocols, with the Moroz-Banaji model interested in the hypoxic insult and the Cloutier model interested in a period of above-average neuronal stimulation.

The question which we are ultimately interested in here is whether the hypoxia model can be improved by addition of some of the features from the Cloutier model. However, here we do not attempt to bring the two models together in anyway, but rather make a simple contribution by briefly exploring the effects of hypoxic conditions in the Cloutier model for the case of the five minute tail pinch experiment.[12]

To this effect, Figure 6 shows the variations of three key chemical species under different arterial oxygen concentrations. From this it appears that neurons and astrocytes may have different thresholds below which their dynamics switch from being relatively normal to being very far from normal. If

[12] As already discussed, the Cloutier model is an inherently dynamic system and thus not well suited to steady-state analysis.

this reflects a physiological truth it would be interesting and would certainly have implications for the hypoxia model, however this prediction has many limitations.

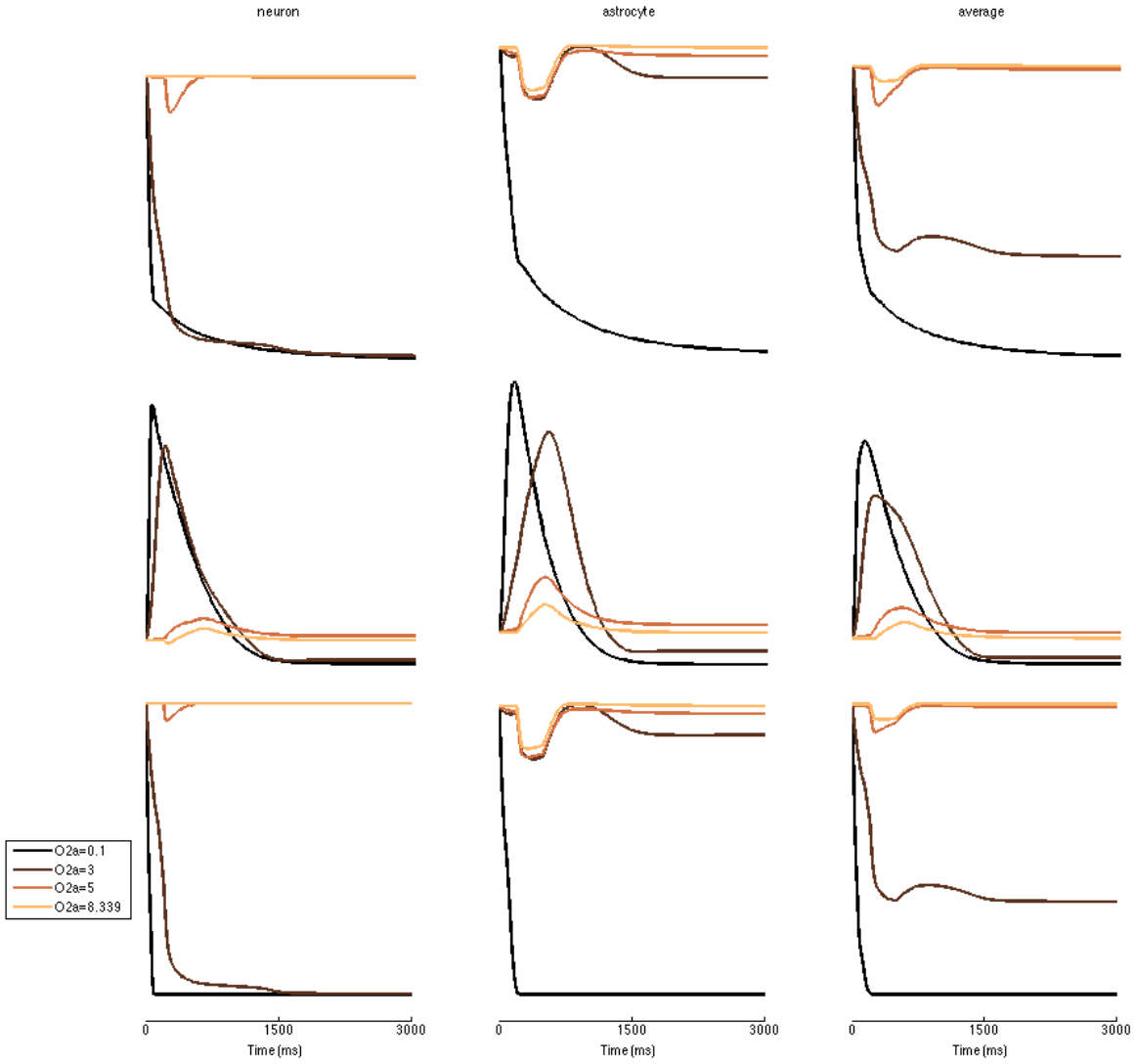

Figure 6: Simulated tail pinch using Cloutier model with different values of O2a (see **legend**, arterial oxygen in mM units). **Top row** shows PCr (phosphocreatine), **second row** shows LAC (lactate), and **bottom row** shows ATP. **Left** is neuron, **centre** is astrocyte, and **right** is volume average (where applicable this includes the extracellular values which are not shown separately).

5 Concluding Remarks

In this work we have introduced a large number of biological concepts any and all of which may play an important role in an accurate model of perinatal hypoxia ischema. In the context of this biological background, we have summarized the properties of two relevant recent models and emphasized the difficulty of comparing them directly. A brief attempt has been made to examine the effect of hypoxia on the neuron-astrocyte interactions, but it is suggested that conclusions should not be drawn until the two models have been fully integrated.

Acknowledgement. The author is grateful to Ilias Tachtsidis, Tracy Moroz, and Tharindi Hapuarachchi for their guidance and technical assistance.

References

[1] N.J. Allen and B.A. Barres. Neuroscience: glia: more than just brain glue. *Nature*, 457(7230):675–677, 2009.

[2] D.V. Azzopardi, B. Strohm, A.D. Edwards, L. Dyet, H.L. Halliday, E. Juszczak, O. Kapellou, M. Levene, N. Marlow, E. Porter, et al. Moderate hypothermia to treat perinatal asphyxial encephalopathy. *New England Journal of Medicine*, 361(14):1349–1358, 2009.

[3] M. Banaji, I. Tachtsidis, D. Delpy, and S. Baigent. A physiological model of cerebral blood flow control. *Mathematical biosciences*, 194(2):125–173, 2005.

[4] N.F. Britton. *Essential mathematical biology*. Springer Verlag, 2003.

[5] T. Çakır, S. Alsan, H. Saybaşılı, A. Akın, and K.Ö. Ülgen. Reconstruction and flux analysis of coupling between metabolic pathways of astrocytes and neurons: application to cerebral hypoxia. *Theoretical Biology and Medical Modelling*, 4(1):48, 2007.

[6] M.E. Clementi, S.G. Condo, M. Castagnola, and B. Giardina. Hemoglobin function under extreme life conditions. *European Journal of Biochemistry*, 223(2):309–317, 1994.

[7] M. Cloutier, F.B. Bolger, J.P. Lowry, and P. Wellstead. An integrative dynamic model of brain energy metabolism using in vivo neurochemical measurements. *Journal of computational neuroscience*, 27(3):391–414, 2009.

[8] P. Dayan. Abbott lf: Theoretical neuroscience. computational and mathematical modeling of neural systems, 2001.

[9] G.A. Dienel. Brain lactate metabolism: the discoveries and the controversies. *Journal of Cerebral Blood Flow & Metabolism*, 2011.

[10] A. Franco Folino. Cerebral autoregulation and syncope. *Progress in cardiovascular diseases*, 50(1):49–80, 2007.

[11] M.R. Freeman and J. Doherty. Glial cell biology in drosophila and vertebrates. *Trends in neurosciences*, 29(2):82–90, 2006.

[12] S. Jacobs, R. Hunt, W. Tarnow-Mordi, T. Inder, and P. Davis. Cooling for newborns with hypoxic ischaemic encephalopathy. *Cochrane Database Syst Rev*, 4(4), 2007.

[13] R. Jolivet, I. Allaman, L. Pellerin, P.J. Magistretti, and B. Weber. Comment on recent modeling studies of astrocyte–neuron metabolic interactions. *Journal of Cerebral Blood Flow & Metabolism*, 30(12):1982–1986, 2010.

[14] Tracy Moroz, Murad Banaji, Nicola J. Robertson, Chris E. Cooper, and Ilias Tachtsidis. Computational modelling of the piglet brain to simulate near-infrared spectroscopy and magnetic resonance spectroscopy data collected during oxygen deprivation. *Journal of The Royal Society Interface*, 2012.

[15] Guillermo Moyna. Bio-chem 341, lecture 36. `http://tonga.usp.edu/gmoyna/biochem341/lecture36.html`, 1999.

[16] David L Nelson and Michael M Cox. *Lehninger Principles of Biochemistry, Fourth Edition*. W. H. Freeman, 2004.

[17] R. Occhipinti, E. Somersalo, and D. Calvetti. Astrocytes as the glucose shunt for glutamatergic neurons at high activity: an in silico study. *Journal of neurophysiology*, 101(5):2528–2538, 2009.

[18] P. Orlowski, M. Chappell, C.S. Park, V. Grau, and S. Payne. Modelling of ph dynamics in brain cells after stroke. *Interface Focus*, 1(3):408–416, 2011.

[19] L. Pellerin. How astrocytes feed hungry neurons. *Molecular neurobiology*, 32(1):59–72, 2005.

[20] L. Pellerin and P.J. Magistretti. Neuroenergetics: calling upon astrocytes to satisfy hungry neurons. *The Neuroscientist*, 10(1):53–62, 2004.

[21] L. Pellerin and P.J. Magistretti. Sweet sixteen for anls. *Journal of Cerebral Blood Flow & Metabolism*, 2011.

[22] L. Pellerin, P.J. Magistretti, et al. Food for thought: challenging the dogmas. *Journal of cerebral blood flow and metabolism: official journal of the International Society of Cerebral Blood Flow and Metabolism*, 23(11):1282, 2003.

[23] Primal Pictures. Cardiovascular system, primalonlinelearning. `http://www.primalonlinelearning.com/cedaandp/caardiovasculat_system/systemic_circulation_vessels_of_head_and_neck.aspx`, 2012.

[24] M. Tsuji, H. Naruse, J. Volpe, D. Holtzman, et al. Reduction of cytochrome aa3 measured by near-infrared spectroscopy predicts cerebral energy loss in hypoxic piglets. *Pediatric research*, 37(3):253, 1995.

[25] R.C. Vannucci et al. Experimental biology of cerebral hypoxia-ischemia: relation to perinatal brain damage. *Pediatric research*, 27(4 Pt 1):317, 1990.

[26] D.D. Wang and A. Bordey. The astrocyte odyssey. *Progress in neurobiology*, 86(4):342–367, 2008.

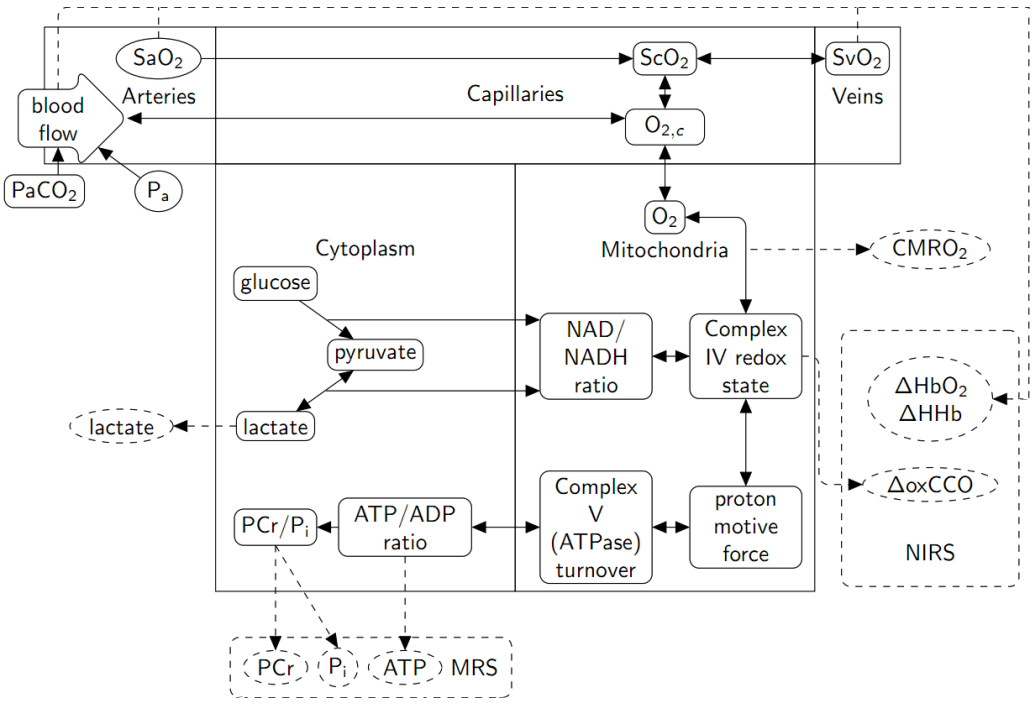

Figure 7: Schematic of the model used in [14] (figure taken directly). See main text for details.

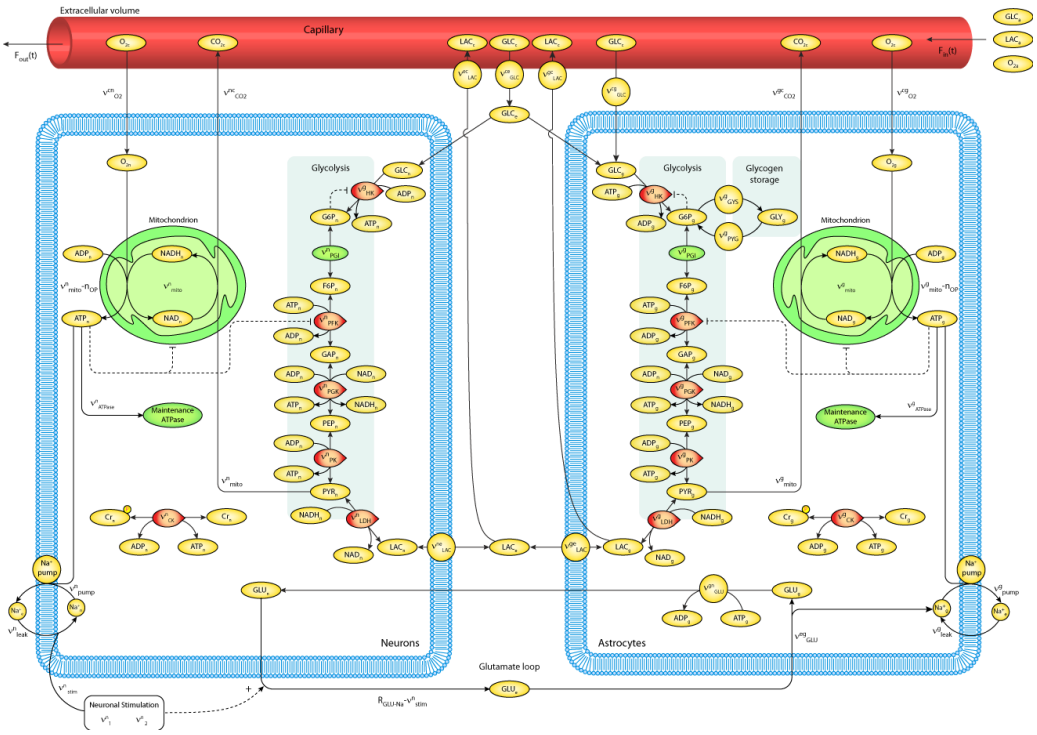

Figure 8: Model used in [7] (figure taken from online material). See main text for details.

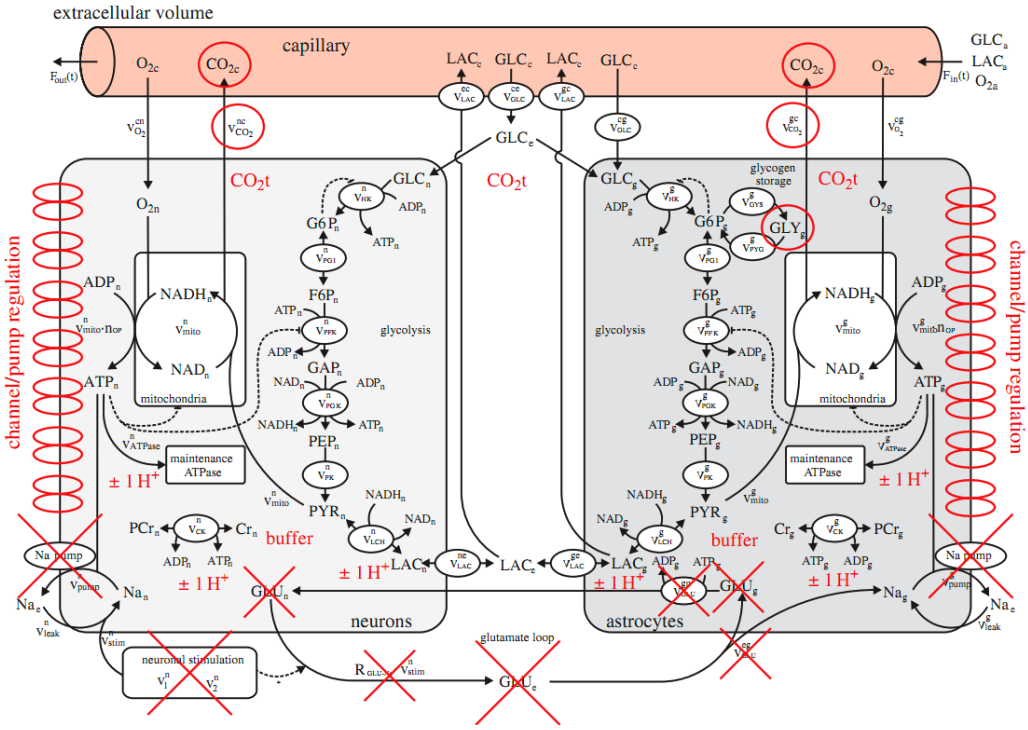

Figure 9: Model used in [18] (figure taken directlyl). See main text for details.

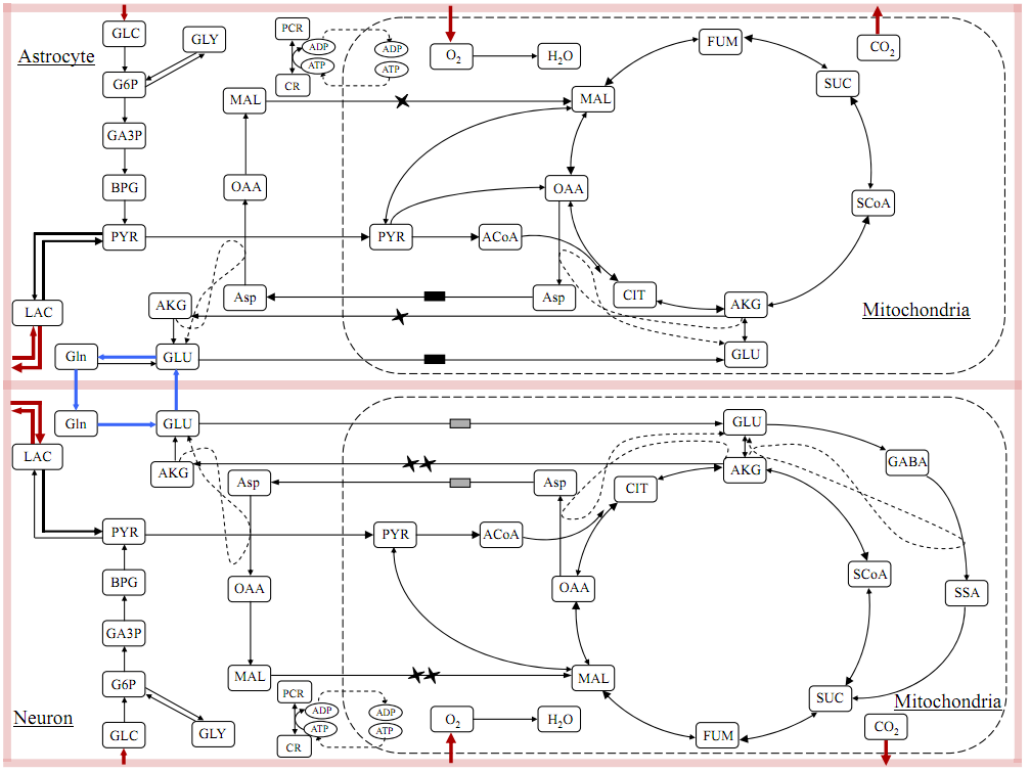

Figure 10: Model used in [17] (figure taken directly). Model consists of extracellular space, neuron, and astrocyte, with the two cells being further divided into cytosol and mitochondrial compartments. Marks on arrows indicate parts of the malate shuttle.

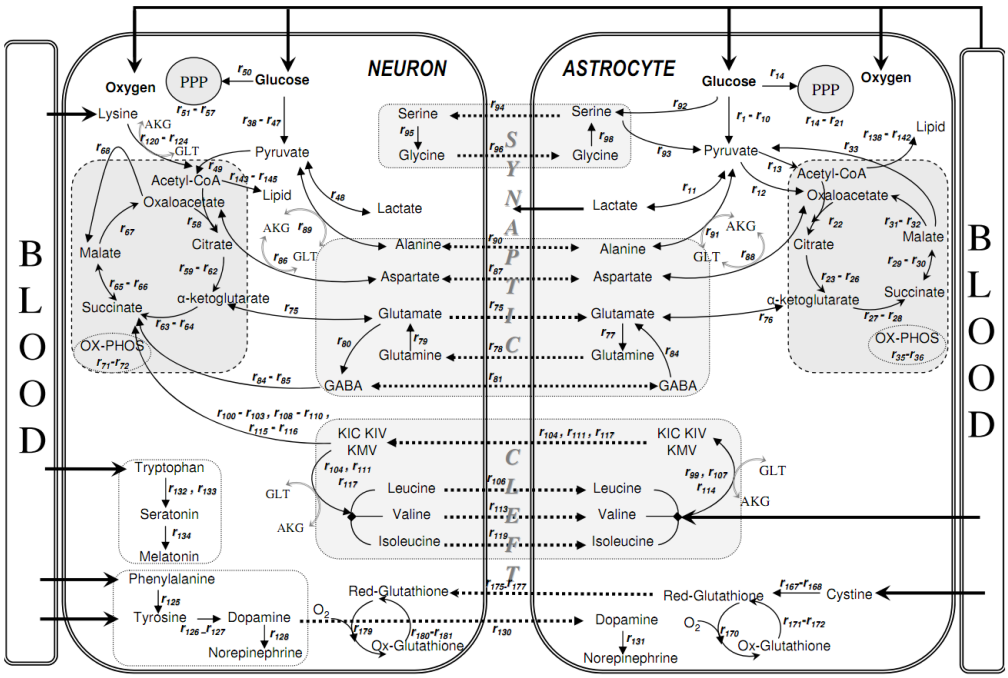

Figure 11: Model used in [5] (figure taken directly). Some details of the model are not depicted here; the full model consists of 78 reactions in the astrocyte, 90 in the neuron and 16 inter-compartmental reactions.